Journal of Engineering Science and Technology
Vol. 10, No.12 (2015) 1525 - 1539
© School of Engineering, Taylor's University

HETEROGENEOUS PHOTOCATALYTIC DEGRADATION OF PHENOL IN AQUEOUS SUSPENSION OF PERIWINKLE SHELL ASH CATALYST IN THE PRESENCE OF UV FROM SUNLIGHT

OSARUMWENSE, J. O.[1,*], AMENAGHAWON, N. A.[2], AISIEN, F. A.[2]

[1]Department of Science Laboratory Technology, Faculty of Life Sciences, University of Benin, P.M.B 1154, Ugbowo, Benin City, Edo State, Nigeria
[2]Department of Chemical Engineering, Faculty of Engineering, University of Benin, P.M.B 1154, Ugbowo, Benin City, Edo State, Nigeria
*Corresponding Author: judeosarumwense@uniben.edu

Abstract

The batch photocatalytic degradation of phenol in aqueous solution was investigated using periwinkle shell ash (PSA) as photocatalyst. Chemical characterisation of the PSA revealed that the major oxides present were calcium oxide (CaO), silica (SiO_2) and aluminium oxide (Al_2O_3) which accounted for 41.3, 33.2 and 9.2% of the weight of PSA characterised. The major elements in PSA were iron (19.2%) and zinc (16.5%). FTIR results revealed absorption peaks of 3626.59 cm^{-1}, 1797.58 cm^{-1}, 1561.43 cm^{-1} and 1374.34 cm^{-1} in the infrared spectrum of PSA corresponding to O–H, C= O, C= C and C–H bonds respectively. Increasing the initial phenol concentration resulted in a decrease in the degradation efficiency of PSA. Lower catalyst loadings favoured the degradation process. Maximum degradation efficiency was obtained when the initial phenol concentration and catalyst loading were set as 50 g/L and 5 g/L respectively. The kinetics of the degradation process was well described by the pseudo first order equation while the diffusion mechanism was well represented by the intra particle diffusion model (R^2>0.90). The adsorption equilibrium data fitted well to the Langmuir isotherm equation with an R^2 value of 0.997.

Keywords: Adsorption capacity, Equilibrium, Phenol, Langmuir-Hinshelwood equation.

1. Introduction

The improper discharge of untreated industrial waste water contaminated with organics poses a problem to the environment [1]. Phenol is a natural as well as a man-made aromatic compound that is predominantly found in wastewater

Nomenclatures

b	Langmuir isotherm parameter, L/mg
C_e	Equilibrium phenol concentration, mg/L
C_o	Initial phenol concentration, mg/L
C_t	Instantaneous phenol concentration, mg/L
k	Pseudo first order model parameter, 1/min
k_2	Pseudo second order model parameter, g/mg.min
k_a	Langmuir-Hinshelwood model parameter, mg/L.min
k_{LH}	Langmuir-Hinshelwood model parameter, L/mg
K_f	Freundlich isotherm parameter, mg/g
n	Freundlich isotherm parameter
r_o	Initial rate of reaction, mg/L.min
R^2	Correlation coefficient
q_e	Equilibrium adsorption capacity, mg/g
q_o	Maximum adsorption capacity, mg/g
q_t	Instantaneous adsorption capacity, mg/g
t	Time, minutes
V_s	Volume of solution, L
W	Catalyst dosage, g/L

Abbreviations

BET	Brunauer Emmet Teller
PSA	Periwinkle Shell Ash
TiO_2	Titanium dioxide
UV	Ultra violet
XRD	X ray diffraction
XRF	X ray fluorescence
ZnO	Zinc oxide

originating from industrial operations such as oil refineries, pesticide and dye manufacture, phenolic resin manufacture, textile, plastic, tanning, rubber, pharmaceuticals, etc. [2-4]. Phenol has been reported to be highly toxic, carcinogenic and resistant to degradation. Hence it is imperative to remove it from wastewater before discharge into natural water bodies [5, 6]. As a result of its relative stability and solubility in water, it is not an easy task to completely remove phenol from wastewater to reach present safety levels in the range of 0.1–1.0 mg L^{-1} [7].

Conventional methods for treating wastewater containing phenolic compounds include chemical coagulation, steam distillation, membrane filtration, electrochemical oxidation, reverse osmosis and adsorption on activated carbon, waste tyre rubber granules, ion exchange resins and silicates [2, 4, 5, 8, 9]. The major drawback of the physical methods amongst these is that they are mere phase transfer processes which results in the generation of more wastes during treatment thus requiring additional treatment steps and cost [10]. Even though the chemical methods appear to be effective, their implementation is usually not economically feasible as the chemicals are required in high dosages [11]. Thus it is imperative to explore other alternative treatment methods. In recent years, heterogeneous photocatalytic degradation which is an advanced oxidation process has emerged as a promising method for the degradation of recalcitrant organic

pollutants in aqueous media. The process is facilitated by semiconductor photocatalysts such as titanium dioxide (TiO_2) and zinc oxide (ZnO) which generate hydroxyl radicals when excited in the presence of ultra violet (UV) radiation [12]. The most significant advantage of this technique is that it can be used to degrade a wide range of toxic organic compounds especially the recalcitrant ones that are not readily amenable to other conventional treatment processes. The products of the degradation process include relatively innocuous simple molecules such as carbon dioxide (CO_2) and water (H_2O) [13]. Furthermore, it is faster than most bioprocesses and cheaper than ozonolysis and radiation based processes as it can be carried out under direct sunlight, making it able to operate independent of any external power source [14]. The sun produces about 0.2 to 0.3 mol photons $m^{-2}h^{-1}$ in the range of 300-400nm with a typical UV flux of 20-30 Wm^2 near the earth's surface. This indicates that sunlight could be an economically suitable source of UV radiation for the process [5].

Amongst the photocatalysts used for photodegradation, TiO_2 and ZnO have received the most attention. This is because of their low cost, high efficiency and quantum yield, resistance to photocorrosion and safe handling [15]. However, certain important deficiencies have been reported to be associated with the use of these catalysts. These deficiencies are related to the limited response and capacity of these catalysts to utilise radiation in the UV region. Hence they require a high power UV excitation source [16]. Furthermore, the recovery potential of the catalysts is limited. It is therefore important to source for alternative photocatalysts with better recovery potential and light absorption capacity, with important focus on locally sourced catalysts.

Periwinkle shell is a waste product generated from the consumption of periwinkle, a small greenish-blue marine snail housed in a V shaped spiral shell [17]. The shells are typically disposed off inappropriately after consuming the edible parts and this contributes to environmental pollution. Some of the uses of periwinkle shells include coarse aggregate in concrete, manufacture of brake pads, paving of water logged areas etc. Nevertheless a large amount of these shells are still discarded annually. Hence it is important to expand the reuse capacity of these shells by utilising them in the production of photocatalysts [13, 18].

The aim of this study was to investigate the potential use of locally sourced periwinkle shell ash for the photocatalytic degradation of phenol in aqueous solution. The effects of initial phenol concentration and catalyst dosage on the degradation process were investigated. The kinetics of the photocatalytic degradation of phenol was modelled using the pseudo first order, pseudo second order, intra particle diffusion and Langmuir-Hinshelwood kinetic models. Isotherm studies were carried out using the Langmuir and Freundlich isotherms equations.

2. Materials and Methods

2.1. Preparation and characterisation of PSA

Periwinkle shells were obtained from Benin City, Edo State of Southern Nigeria. All reagents used were of analytical grade and were obtained from Rovet scientific Limited, Benin City, Edo State, Nigeria. The shells were washed and dried in an oven at 110°C to constant mass, followed by crushing and calcination at 600°C in a muffle furnace and subsequent sieving to obtain fine particles (<

350µm) of periwinkle shell ash (PSA) [13]. The prepared PSA was characterised by determining its composition using X-Ray Fluorescence (XRF) analysis. X-ray diffraction (XRD) was used to determine the ultimate elemental composition of the PSA using a Philips X-ray diffractometer [13]. Fourier transform infrared spectrometry (FTIR) was also carried out on the PSA and the IR spectra were recorded using Perkin Elmer spectrum 100 FT–IR spectrometer in the frequency range 4000 to 400cm^{-1}, operating in ATR (attenuated total reflectance) mode. The surface structure of the PSA was evaluated by nitrogen adsorption method at -196ºC. The surface area of the PSA was determined using the standard BET equation [13]. Other properties such as bulk density and porosity were determined using standard methods.

2.2. Preparation of phenol solution

Analytical reagent grade phenol was used in this study. A stock solution of phenol was prepared by dissolving an appropriate amount of phenol in 1000 mL of deionised water. Working solutions with different concentrations of phenol were prepared by appropriate dilutions of the stock solution with deionised water immediately prior to their use.

2.3. Photocatalytic degradation studies

All the photocatalytic degradation experiments were carried out under atmospheric conditions in mechanically agitated 500 mL Erlenmeyer flasks under visible light. A 14 cm focal length converging lens was used to direct the rays of sunlight on to the reaction vessel. The sunlight experiments were carried out between 12:00 P.M to 3:00 P.M. on a sunny day. The light intensity was measured using UV-light intensity detector (Lutron UV-340), which was found to be in the range of 0.370 to 0.480 mW/cm^2. For each experiment, a predetermined amount of PSA catalyst was added to the phenol solution and the suspension was magnetically stirred without any permanent air bubbling. The temperature was maintained at 32 ±2°C and monitored throughout the process [18]. The study was also carried out in the absence of light and catalyst to check if there was any change in the degradation of the sample. The effects of initial phenol concentration and PSA dosage on the degradation efficiency were investigated. At the end of each experiment the agitated suspension mixture was filtered using a 0.45 µm membrane and the residual concentration of phenol was determined using a UV-Vis spectrophotometer (T70, PG Instrument). The percentage photocatalytic degradation of phenol was calculated using the equation.

$$Degradation\ efficiency = \frac{C_o - C_t}{C_o} \times 100 \quad (1)$$

The amount of phenol adsorbed at time *t,* (q_t) and at equilibrium (q_e) were calculated using the equations.

$$q_t = \frac{V_s(C_o - C_t)}{W} \quad (2)$$

$$q_e = \frac{V_s(C_o - C_e)}{W} \quad (3)$$

where C_o, C_e and C_t are the initial, equilibrium and instantaneous phenol concentrations respectively. V_s is the volume of the aqueous solution and W is the amount of catalyst.

3. Results and Discussion

3.1. Characterisation of PSA

The results of the chemical characterisation of the PSA used in this study have been previously reported by Aisien et al. [13]. According to them, the XRF results showed that the major oxides present in the PSA were calcium oxide (CaO), silica (SiO_2) and aluminium oxide (Al_2O_3) which accounted for 41.3, 33.2 and 9.2% of the weight of PSA characterised. It was reported by Navaladian et al. [19] that transition metals in their oxide form are known to exhibit catalytic action. The XRD results showed that the major elements in PSA were iron (19.2%) and zinc (16.5%). The FTIR results revealed absorption peaks of 3626.59 cm^{-1}, 1797.58 cm^{-1}, 1561.43 cm^{-1} and 1374.34 cm^{-1} in the infrared spectrum of periwinkle shell ash corresponding to O–H, C= O, C= C and C–H bonds respectively. These FTIR bands represent functional groups that possess strong bonds which can be protonated at slightly acidic solution to be potential adsorption sites for organic molecules [20].

3.2. Preliminary studies to determine the effect of UV radiation

The results of preliminary studies carried out to determine the effect of UV radiation on the photodegradation process is presented in Fig. 1. One set of the experiments was performed with phenol solution mixed with periwinkle shell ash and exposed to sunlight, the second set was carried out in the absence of sun light (physical adsorption), and the third set was carried out by exposing phenol solution to sunlight without the periwinkle shell ash.

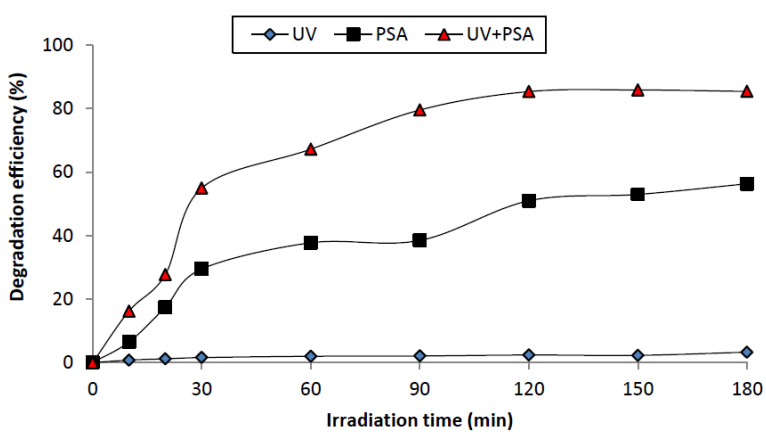

Fig. 1. Results of preliminary studies to determine effect of UV radiation.

Some level of degradation, though not very significant was observed when the degradation experiments were carried out in the presence of UV alone. The degradation efficiency was observed to improve when the same experiments were

facilitated with PSA without UV. This suggests that the level of degradation recorded could have resulted from physical adsorption of the phenol molecules onto the surface of the PSA particles. The degradation efficiency was significantly improved when PSA was used in the presence of UV. This shows the importance of UV radiation to the photodegradation process. Similar observations were reported by Hussein et al. [21] who investigated the photocatalytic degradation of thymol blue in the presence of UV from sunlight. Zahraa et al. [22] reported that the efficiency of the photocatalyst in the presence of UV from sunlight has to do with the activation of the active sites on the catalyst surface when it absorbs photons from sunlight. The electron-hole pairs generated by the activated catalyst sites are responsible for the oxidation of the organic pollutant during photodegradation [23].

3.3. Effect of initial phenol concentration

The initial concentration of organic pollutants in contaminated water is a significant parameter that affects the efficiency of the treatment process [24]. The time dependent concentration profile of phenol during photodegradation as presented in Fig. 2 shows that the concentration of phenol decreased with time in the course of the treatment process. This suggests that the phenol molecules were being degraded as the photocatalytic reaction progressed. The results also show that as the initial phenol concentration was increased from 50 to 400 mg/L, the degradation efficiency of periwinkle shell ash decreased. This phenomenon is due to the decrease in the relative ratio of the hydroxyl radicals to the molecules of the organic contaminants in the solution as suggested by Hashim et al. [25]. They further stated that when the concentration of the pollutant increases, the amount of the molecule adsorbed onto the surface of the catalyst also increases resulting in fewer active sites for reaction. Also, as the concentration of the compound increases, the solution becomes more turbid thereby reducing the amount of photons that get to the catalyst surface and as a result, the amount of hydroxyl radicals attacking the organic molecules becomes limited thus reducing the degradation efficiency [26, 27].

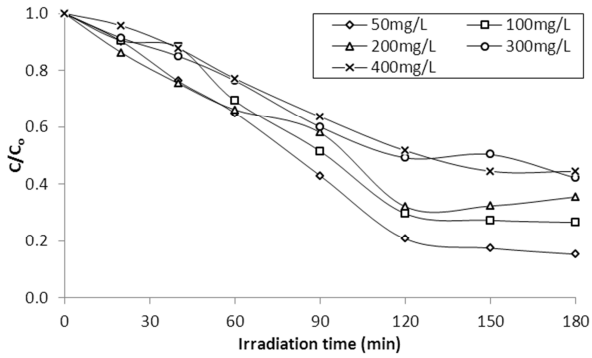

Fig. 2. Effect of initial phenol concentration on the photodegradation of phenol by PSA.

3.4. Effect of catalyst loading

Figure 3 shows the effect of catalyst loading on the photodegradation process. The results show that the percentage of phenol degraded increased with increasing catalyst loading up to 5g/L of PSA and thereafter decreased with increasing PSA loading. The initial increase in degradation efficiency observed might be due to the increase in the number of active sites on the photocatalyst surface [28, 29]. The decrease in degradation efficiency observed beyond a catalyst loading of 5 g/L could be attributed to the increase in the turbidity of the solution as a result of the excess catalyst present in the degradation reaction vessel. This leads to the so called screening effect that involves the reflectance, interception and scattering of light and hence a fraction of the available light rays do not penetrate into the solution [27, 30]. A similar behaviour was observed by Hashim et al. [25] who reported that in batch or dynamic flow photoreactors, the initial reaction rates are directly proportional to the catalyst loading indicating a true heterogeneous catalytic regime, but above a certain loading limit, the reaction rate levels off and further increase in catalyst loading does not benefit the process. So et al. [31] suggested that agglomeration and sedimentation of the catalyst particles at high catalyst loading could also be responsible for the decrease in degradation efficiency.

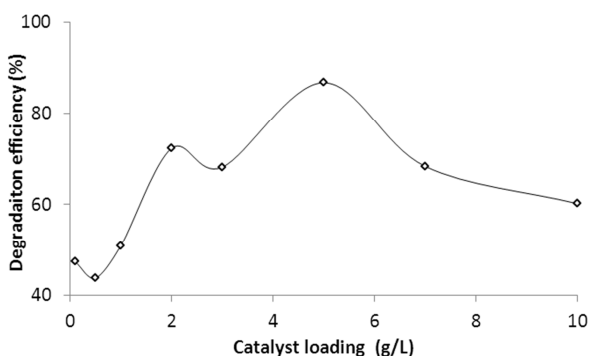

Fig. 3. Effect of catalyst loading on the photodegradation of phenol by PSA.

3.5. Kinetics of photodegradation of phenol

Kinetic data of degradation of phenol were analysed using apparent pseudo first order, pseudo second order, intra-particle diffusion and Langmuir-Hinshelwood kinetic models.

3.5.1. Apparent pseudo first order model

The apparent pseudo first order equation is generally expressed as:

$$\frac{dC}{dt} = kC \tag{4}$$

The integrated linear form of the pseudo first order model equation is presented as follows:

$$\ln \frac{C_o}{C} = kt \tag{5}$$

C_o is initial concentration of phenol; k (min^{-1}) is the pseudo first order rate constant. The plot of ln C_o/C versus t resulted in a linear relationship from which k was determined from the slope of the graph as shown in Fig. 4. The kinetic parameters and the R^2 value of the pseudo first order rate equation as obtained from Fig. 4 is shown in Table 1.

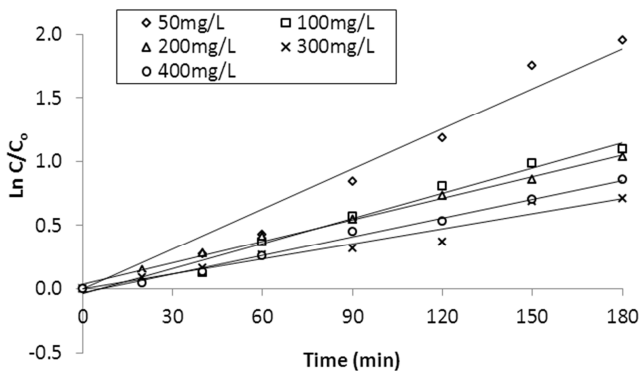

Fig. 4. Pseudo first order kinetic plot for the degradation of phenol by PSA.

3.5.2. Pseudo second order model

The pseudo second order kinetic equation and its integrated linear form are expressed in Eqs. (6) and (7) respectively [32].

$$\frac{dq_t}{dt} = k_2 (q_e - q_t)^2 \tag{6}$$

$$\frac{t}{q_t} = \frac{1}{k_2 q_e^2} + \frac{1}{q_e} t \tag{7}$$

where k_2 ($gmg^{-1}min^{-1}$) is the pseudo second order rate constant. The plot of (t/q_t) versus t is shown in Fig. 5. The kinetic constants calculated from the plot at different initial phenol concentrations are shown in Table 1. It was observed that the model was able to describe the kinetics of the process as seen from the relatively high R^2 values. However, it was also observed that the R^2 values for each concentration value for the case of the pseudo first order kinetic model were much higher than those of the pseudo second order kinetic model. Theoretically, when the R^2 value is nearer to 1.0, the fit of data is considered to be excellent. This suggests that the present photodegradation system was better represented by the pseudo first order model than the pseudo second order model.

As shown in Table 1, the rate constant of the apparent pseudo first order equation decreased from 0.011 to 0.004 min^{-1} as the initial concentration increase from 50 to 400 mg/L. This is an indication that increasing the initial phenol concentration did not

have a positive effect on the rate of the degradation process. In fact, this corroborates the observation reported in Fig. 2. According to Daneshvar et al. [33], a decrease in rate constant may be as a result of the decrease in the number of active sites on the catalyst surface. It was however observed that the rate constant remained unchanged between 300 and 400mg/L; this might be an indication that 300 mg/L may be the maximum concentration of phenol that can be easily degraded by PSA.

3.5.3. Intra particle diffusion model

The intra particle diffusion kinetic model is written as follows [34]:

$$q_t = K_p t^{1/2} + C \tag{8}$$

Here K_P (mg/gmin^{½}) is the intra particle diffusion rate constant. C is a measure of boundary layer effect. The value of C indicates the contribution of the surface sorption to the rate controlling step. The intra-particle diffusion model proposed has been widely applied for the analysis of adsorption kinetics. According to the model, a plot of q_t versus $t^{1/2}$ should be a straight line from the origin if the adsorption mechanism follows the intra-particle diffusion process only. Figure 6 shows straight line plots for the range of phenol concentration investigated which indicates that the adsorption data fitted the intra-particle diffusion model. Furthermore, the results show that intra-particle diffusion might not be rate controlling as there was some boundary layer effect observed [35, 36].

Table 1. Kinetic parameters of pseudo first order, pseudo second order, intra particle diffusion and Langmuir-Hinshelwood models.

Kinetic models	Initial concentration of phenol mg/L				
	50	100	200	300	400
Pseudo first order					
***k* (1/min)**	0.011	0.006	0.005	0.004	0.004
R^2	0.982	0.984	0.995	0.951	0.992
Pseudo second order					
k_2 **(g/mg/min)**	5.9×10^{-3}	1.2×10^{-3}	6.7×10^{-4}	4.0×10^{-4}	5.6×10^{-3}
q_e **(mg/g)**	1.51	3.57	6.37	9.52	15.60
R^2	0.944	0.584	0.786	0.859	0.953
Intra particle diffusion					
K_P**(g/mg/min$^{1/2}$)**	0.072	0.120	0.214	0.300	0.358
R^2	0.980	0.957	0.966	0.969	0.925
Langmuir-Hinshelwood					
k_a **(L/mg)**			0.0143		
k_{LH} **(Lmin^{-1})**			1.447		
R^2			0.809		

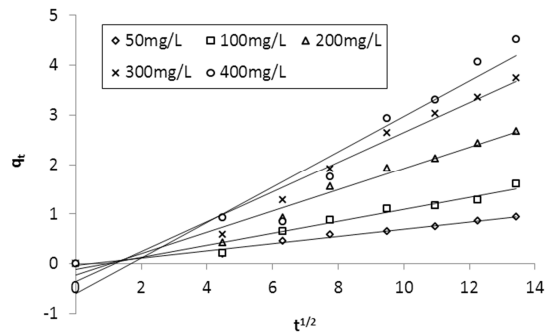

Fig. 6. Intra particle diffusion kinetic plot for the degradation of phenol by PSA.

3.5.4. Langmuir-Hinshelwood model

The Langmuir-Hinshelwood mechanism is a common kinetic model where the attack of the target organic molecules takes place on the catalyst surface [37]. The simplest form of Langmuir-Hinshelwood model equation is expressed as follows:

$$r_o = \frac{k_{LH} k_a C_o}{1 + k_a C_o} \tag{9}$$

r_o is the rate of disappearance of organic substrate, k_a is equilibrium constant for adsorption of substrate onto adsorbent, C_o is the initial concentration of substrate and k_{LH} is the limiting reaction rate constant. The linearised form of Equation (9) is given as:

$$\frac{1}{r_o} = \frac{1}{k_{LH} k_a} \frac{1}{C_{eq}} + \frac{1}{k_{LH}} \tag{10}$$

The kinetic data were analysed to understand the dynamics of the reaction and adsorption processes in terms of the rate constant and capacity of phenol degraded. The values of k_a and k_{LH} as obtained from Fig. 7 are given in Table 1. The value of k_a indicates high affinity between the phenol molecules and the surface of PSA.

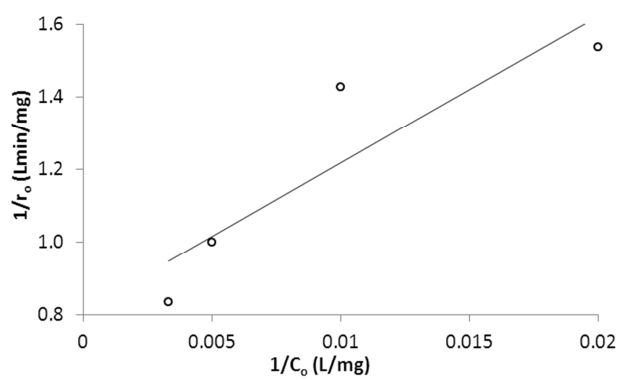

Fig. 7. Langmuir-Hinshelwood kinetic plot for the degradation of phenol by PSA.

3.6. Equilibrium studies

The equilibrium adsorption isotherm is fundamentally important in the design of adsorption systems. Equilibrium relationships between adsorbent and adsorbate are described by adsorption isotherms, usually the Langmuir and Freundlich isotherms.

3.6.1. Langmuir isotherm

The Langmuir theory assumes that adsorption occurs at specific homogeneous sites within the adsorbent [38]. The Langmuir isotherm is expressed as follows:

$$q_e = q_m \left(\frac{bC_e}{1+bC_e} \right) \tag{11}$$

q_m (mg/g) is the maximum adsorption capacity of the photocatalyst, q_e (mg/g) is the adsorption capacity of the photocatalyst at equilibrium, b (L/mg) is the Langmuir equilibrium constant related to the affinity of the binding site and C_e (mg/L) is the concentration of the substrate in aqueous solution at the equilibrium. The linear transformation of Equation (11) can be expressed as follows:

$$\frac{C_e}{q_e} = \frac{1}{q_m} C_e + \frac{1}{bq_m} \tag{12}$$

A linear plot of C_e/q_e against C_e as shown in Fig. 8 was employed to obtain the values of q_m and b from the slope and intercept of the plot respectively. The values of the Langmuir isotherm parameters as well as the correlation coefficient (R^2) of the Langmuir equation are given in Table 2. The type of adsorption can be determined by using a dimensionless separation factor (R_L) which can be expressed as:

$$R_L = \frac{1}{1+bC_o} \tag{13}$$

R_L can be used to interpret the sorption type given as unfavourable ($R_L > 1$), favourable ($0<R_L<1$), linear ($R_L = 1$) and irreversible ($R_L = 0$).

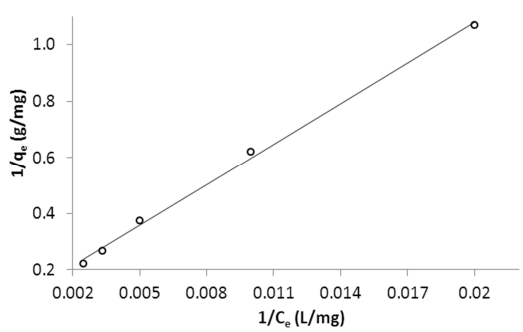

Fig. 8. Langmuir isotherm equation fitted to batch equilibrium data of phenol degradation.

Table 2. Parameters of Langmuir and Freundlich isotherm equations.

Langmuir Isotherm			Freundlich Isotherm		
q_m	b	R^2	K_f	n	R^2
8.55	0.0024	0.997	0.041	1.185	0.992

Table 3. R_L values and type of isotherm.

Initial concentration (mg/L)	R_L Value
50	0.909
100	0.833
200	0.714
300	0.625
400	0.556

For this study, the values of R_L given in Table 3 are between zero and one indicating that the adsorption was favourable.

3.6.2. Freundlich isotherm

The Freundlich model describes multilayer adsorption onto heterogeneous surfaces as opposed to monolayer adsorption onto homogeneous surfaces according to the Langmuir model. The empirical form of the Freundlich equation is given by:

$$q = K_f C^{1/n} \tag{14}$$

q (mg/g) is the adsorbed amount, C (mg/L) is the remaining adsorbate concentration and K_f and n are constants. The linearised form of Eq. (14) is given as:

$$\log q_e = \log K_f + 1/n \log C_e \tag{15}$$

A linear plot of $log\ q_e$ against $log\ C_e$ as shown in Fig. 9 was employed to obtain the values of K_f and n from the intercept and slope of the plot respectively. The values of these parameters as well as the correlation coefficient (R^2) of the Freundlich equation are given in Table 2. Figures 8 and 9 as well as the information presented in Table 2 show that the adsorption process of phenol fitted well to the Langmuir and Freundlich isotherm models. However, the higher correlation coefficient value of 0.997 suggests that the Langmuir isotherm might be a more suitable isotherm model. It was thus concluded that the adsorption process of phenol onto PSA catalyst exhibited monolayer adsorption and the maximum monolayer adsorption capacity were found to be 8.55 mg/g.

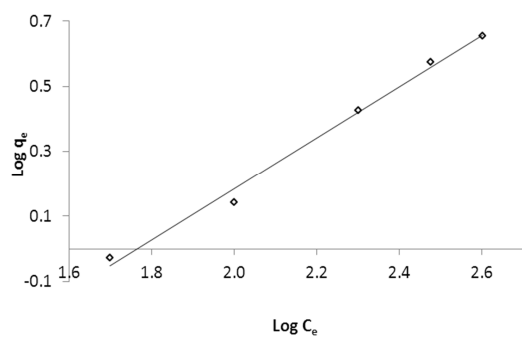

Fig. 9. Freundlich isotherm equation fitted to batch equilibrium data of phenol degradation.

4. Conclusions

The potential use of periwinkle shell ash as photocatalyst for the heterogeneous photocatalytic degradation of phenol was investigated in this study. The following conclusions can be drawn from this study.

- Solar irradiation is effective in the degradation of phenol using periwinkle shell ash photocatalyst
- Periwinkle shell ash possesses functional groups that have high adsorption affinity for organic compounds as evident from the FTIR results
- Increasing the initial concentration phenol does not impact positively on the efficiency of the degradation process
- Low catalyst loading favours the degradation process
- The reaction kinetics for the degradation process fitted more to pseudo first order than second order model equation and the diffusion mechanism was well represented by the intra particle diffusion model
- The adsorption equilibrium was well described by the Langmuir isotherm equation indicating mono layer type adsorption.

References

1. Radcliff, J.C. (2006). Future directions for water recycling in Australia. *Desalination*, 187(1-3), 77-87.
2. Aisien, F.A.; Amenaghawon, N.A.; and Adeboyejo, A.R. (2013). Application of recycled rubber from scrap tire in the removal of phenol from aqueous solution. *Pacific Journal of Science and Technology*, 14(2), 330-341.
3. Manojlovic, D.; Ostojic, D.R.; Obradovic, B.M.; Kuraica, M.M.; Krsmanovic, V.D.; and Puric, J. (2007). Removal of phenol and chlorophenols from water by new ozone generator. *Desalination*, 213(1-3), 116-122.
4. Nagda G.K.; Diwan A.M.; and Ghole V.S. (2007). Potential of tendu leaf refuse for phenol removal in aqueous system. *Applied Ecology and Environmental Research*, 5(2), 1-9.
5. Ahmed, S.; Rasul, M.G.; Martens, W.N.; Brown, R.J.; and Hashib, M.A. (2010). Heterogeneous photocatalytic degradation of phenols in wastewater: a review on current status and developments. *Desalination*, 261(1-2), 3-18.
6. Eriksson, E.; Baun, A.; Mikkelsen, P.S.; and Ledin, A. (2007). Risk assessment of xenobiotics in stormwater discharged to Harrestup A^{o}, Denmark. *Desalination*, 215(1-3), 187-197.
7. Azevedo, E.B.; Tôrres, A.R.; Aquino Neto, F.R.; and Dezotti M. (2009). TiO_2 photocatalysed degradation of phenol in saline media in an annular reactor: hydrodynamics, lumped kinetics, intermediates, and acute toxicity. *Brazilian Journal of Chemical Engineering,* 26(1), 75-87.
8. Carmona, M.; De Lucas, A.; Valverde, J.L.; Velasco, B.; and Rodriguez, J.F. (2006). Combined adsorption and ion exchange equilibrium of phenol on Amberlite IRA-420. *Chemical Engineering Journal*, 117(2), 155-160.
9. Goncharuk V.V.; Kucheruk D.D.; Kochkodan V.M.; and Badekha V.P. (2002). Removal of organic compounds from aqueous solutions by reagent enhanced reverse osmosis. *Desalination*, 143(1), 45-51.
10. Bergamini, R.; Azevedo, E.B.; and Araújo, L.R. (2009). Heterogeneous photocatalytic degradation of reactive dyes in aqueous TiO_2 suspensions: Decolourisation kinetics. *Chemical Engineering Journal*, 149(1), 215-220.

11. Robinson, T.; McMullan, G.; Marchant, R.; and Nigam, P. (2001). Remediation of dyes in textile effluent: a critical review on current treatment technologies with a proposed alternative. *Bioresource Technology*, 77(3), 247-255.
12. Akyol, A.; and Bayramoglu, M. (2008). The degradation of an azo dye in a batch slurry photocatalytic reactor. *Chemical Engineering and Processing: Process Intensification*, 47(12), 2150-2156.
13. Aisien, F.A.; Amenaghawon, N.A.; and Assogba, M.M. (2014). Heterogeneous photocatalytic degradation of naphthalene using periwinkle shell ash: Effect of operating variables, kinetic and isotherm study. *South African Journal of Chemical Engineering*, 19(1), 31-45.
14. Lair, A.; Ferronato, C.; Chovelon, J.M.; and Herrmann, J.M. (2008). Naphthalene degradation in water by heterogeneous photocatalysis: an investigation of the influence of inorganic anions. *Journal of Photochemistry and Photobiology A: Chemistry*, 193(2), 193-203.
15. Ahmed, S.; Rasul, M.G.; Martens, W.N.; Brown, R.; and Hashib, M.A. (2011). Advances in heterogeneous photocatalytic degradation of phenols and dyes in wastewater: a review. *Water, Air, & Soil Pollution*, 215(1-4), 3-29.
16. Liu, G.; Wang, Z.; Zheng, W.; Yang, S.; and Sun, C. (2014). Visible-light-driven photocatalytic degradation of aniline over $NaBiO_3$. *Advances in Condensed Matter Physics*, Article ID 961609, 5 pages.
17. Olutoge, F.A.; Okeyinka, O.M.; and Olaniyan, O.S. (2012). Assessment of the suitability of periwinkle shell ash (PSA) as partial replacement for ordinary Portland cement (OPC) in concrete. *International Journal of Research and Reviews in Applied Sciences*, 10(3), 428-434
18. Aisien, F.A.; Amenaghawon, N.A.; and Ekpenisi, E.F. (2013). Photocatalytic decolourisation of Industrial wastewater from a soft drink company. *Journal of Engineering and Applied Sciences*, 9, 11-16.
19. Navaladian, S.; Janet, C.M.; Viswanathan, B.; and Viswanath, R.P. (2007). *On the possible treatment procedures for organic contaminants*. In: Kaneco S, Viswanathan B, Katsumata H. eds. Photo/electrochemistry & Photobiology in the Environment, Energy and Fuel, pp. 1-51.
20. Royer, B.; Cardoso, N.F.; Lima E.C.; Vaghetti, J.C.P.; Simon, N.M.; Calvere T.; and Veses, R.C. (2009). Application of Brazilian pine-fruit shell in natural and carbonized forms as adsorbents to removal of methylene blue from aqueous solutions – Kinetic and equilibrium study, *Journal of Hazardous Materials*, 164(2-3), 1213–1222.
21. Hussein, F.H.; Alkhateeb, A.N.; and Ismail, J.K. (2008). Solar photolysis and photocatalytic decolourization of thymol blue. *E-Journal of Chemistry*, 5(2), 243-250.
22. Zahraa, O.; Marie, S.; Evenou, F.; Hachem, C.; Pons, M.N.; Alinsafi, M.; and Bouchy, M. (2006). Treatment of wastewater dyeing agent by photocatalytic process in solar reactor. *International Journal of Photoenergy*, 8(3), 2006, 1-9.
23. Poulios, I.; Micropoulou, E.; Panou, R.; and Kostopoulou, E. (2003). Photooxidation of eosin Y in the presence of semiconducting oxides. *Applied Catalysis B: Environmental*, 41(4), 345-355.

24. Hong, S.S.; Ju, C.S.; Lim, C.G.; Ahn, B.H.; Lim, K.T.; and Lee, G.D. (2001). A photocatalytic degradation of phenol over TiO2 prepared by sol-gel method. *Journal of Industrial and Engineering Chemistry*, 7(2), 99-104.
25. Hashim, H.A.A.; Mohamed, A.R.; and Lee, K.T. (2012). Solar photocatalytic degradation of tartrazine using titanium dioxide. *Jurnal Teknologi*, 35(1), 31-40.
26. Akyol, A.; Yatmaz, H.C.; and Bayramoglu, M. (2004). Photocatalytic decolorization of remazol red RR in aqueous ZnO suspensions. *Applied Catalysis B: Environmental*, 54(1), 19-24.
27. Byrappa, K.; Subramani, A.K.; Ananda, S.; Rai, K.L.; Dinesh, R.; and Yoshimura, M. (2006). Photocatalytic degradation of rhodamine B dye using hydrothermally synthesized ZnO. *Bulletin of Materials Science*, 29(5), 433-438.
28. Akpan, U.G.; and Hameed, B.H. (2009). Parameters affecting the photocatalytic degradation of dyes using TiO_2-based photocatalysts: A review. *Journal of Hazardous Materials*, 170(2-3), 520-529.
29. Inamdar, J.; and Singh, S.K. (2008). Photocatalytic detoxification method for zero effluent discharge in dairy industry: Effect of operational parameters. *International Journal of Chemical and Biological Engineering*, 1(4), 160-164.
30. Saquib, M.; Tariqa, M.A.; Faisala, M.; and Muneer, M. (2008). Photocatalytic degradation of two selected dye derivatives in aqueous suspensions of titanium dioxide. *Desalination*, 219(1-3), 301-311.
31. So, C.M.; Cheng, M.Y.; Yu, J.C.; and Wong, P.K. (2002). Degradation of azo dye procion red MX-5B by photocatalytic oxidation. *Chemosphere*, 46(6), 905-912.
32. Ho, Y. S.; and McKay, G. (1999). Pseudo-second order model for sorption processes. *Process Biochemistry*, 34(5), 451-465.
33. Daneshvar, N.; Aber, S.; Dorraji, M.S.; Khataee, A.R. and Rasoulifard, M.H. (2008). Preparation and investigation of photocatalytic properties of ZnO nanocrystals: effect of operational parameters and kinetic study. *International Journal of Chemical, Nuclear, Metallurgical and Materials Engineering*, 1(5), 66-71.
34. Weber W.J.; and Morris, J. C. (1963). Kinetics of adsorption on carbon from solution. *Journal of the Sanitary Engineering*, 89(2), 31-60.
35. Akar, S.T.; Gorgulu, A.; Kaynak, Z.; Anila, B.; Akar, T. (2009). Biosorption of Reactive Blue 49 dye under batch and continuous mode using a mixed biosorbent of macro fungus Agaricus bisporus and Thuja orientalis cones. *Chemical Engineering Journal,* 148(1), 26-34.
36. Tsai, W.T.; Hsien, K.J.; and Yang, J.M. (2004). Silica adsorbent prepared from spent diatomaceous earth and its application to removal of dye from aqueous solution. *Journal of Colloid and Interface Science*, 275(2), 428-433.
37. Turchi, C.S.; and Ollis, D.F. (1990). Photocatalytic degradation of organic water contaminants: mechanisms involving hydroxyl radical attack. *Journal of Catalysis*, 122(1), 178-192.
38. Langmuir, I. (1918). The adsorption of gases on plane surfaces of glass, mica and platinum. *Journal of American Chemical Society*, 40(9), 1361-1403.